High Altitude Aerosol Chemical Characterization and Source Identification: Insights from the CALISHTO Campaign

Olga Zografou[1,2], Maria Gini[1], Prodromos Fetfatzis[1], Konstantinos Granakis[1], Romanos Foskinis[1,3,8], Manousos Ioannis Manousakas[1,4], Fotios Tsopelas[2], Evangelia Diapouli[1], Eleni Dovrou[5,6], Christina N. Vasilakopoulou[5,6], Alexandros Papayannis[3], Spyros N. Pandis[5,6], Athanasios Nenes[7,8], and Konstantinos Eleftheriadis[1]

[1]Environmental Radioactivity & Aerosol Tech. for Atmospheric & Climate Impacts, INRaSTES, National Centre of Scientific Research "Demokritos", Ag. Paraskevi, 15310, Greece
[2]Laboratory of Inorganic and Analytical Chemistry, School of Chemical Engineering, National Technical University of Athens, Athens, Greece
[3]Laser Remote Sensing Unit, Physics Department, School of Applied Mathematics and Physical Sciences, National and Technical University of Athens, 15780 Zografou, Greece
[4]Laboratory of Atmospheric Chemistry, Paul Scherrer Institute, CH-5232, Villigen PSI, Switzerland
[5]Institute of Chemical Engineering Sciences, ICE-HT, Patras, 26500, Greece
[6]Department of Chemical Engineering, University of Patras, Patras, 26504, Greece
[7]Institute for Chemical Engineering Sciences, Foundation for Research and Technology, Patras, Greece
[8]School of Architecture, Civil and Environmental Engineering, École Polytechnique Fédérale de Lausanne, Lausanne, Switzerland

Correspondence to: Konstantinos Eleftheriadis (elefther@ipta.demokritos.gr) and Olga Zografou (o.zografou@ipta.demokritos.gr)

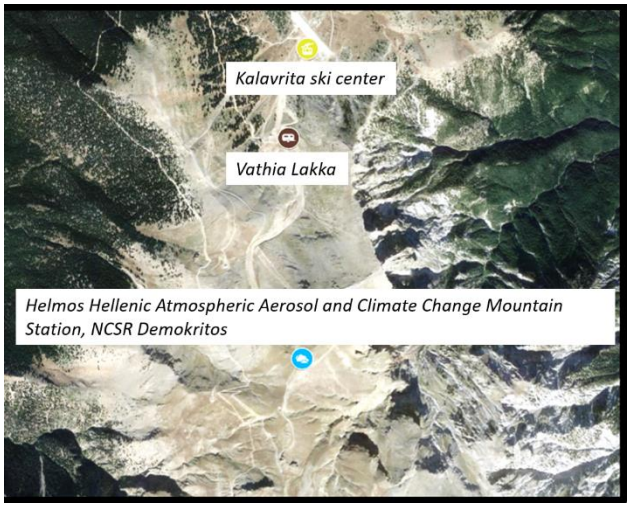

Figure S1. The Helmos Hellenic Atmospheric Aerosol and Climate Change (HAC)^2 station in Helmos Mt. (GAW, ACTRIS, and PANACEA). The maps were obtained from © Google Maps (maps.google.com) Imagery 2023 Terrametrics, Mapdata 2023 and modified by the authors.

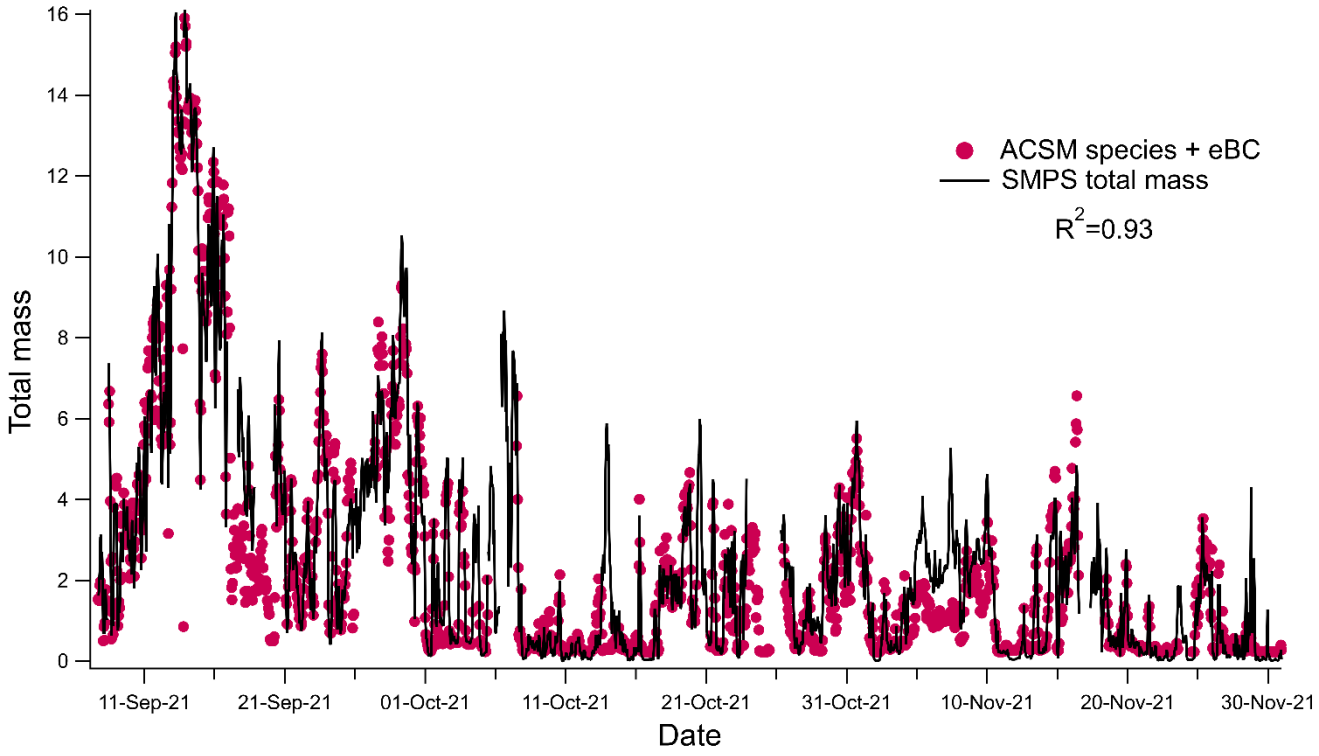

Figure S2. Time series and correlation coefficient between the sums of the ACSM plus *eBC* mass vs the total SMPS PM_1 mass using the collection efficiency of 0.28.

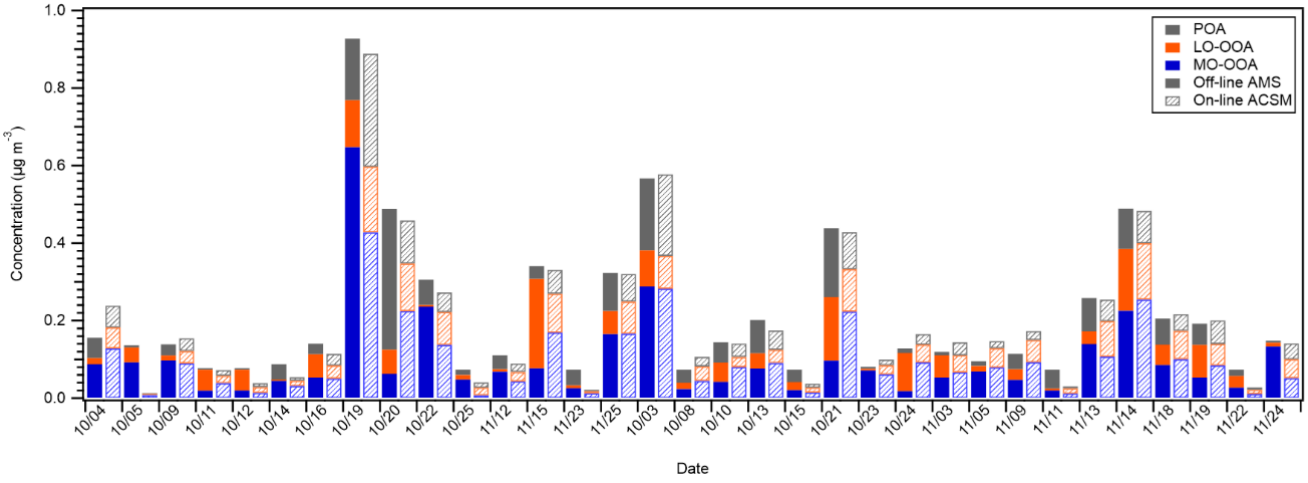

Figure S3. Absolute concentrations of each factor from PMF analysis on the organic fraction by the two methods (off-line AMS and online ACSM). The absolute off-line AMS concentrations were estimated from the percent contribution of each factor from the off-line analysis and the OA concentration reported by the on-line ACSM for each day.

Section S1. Off-line AMS analysis on filters and PMF analysis on AMS dataset.

Filter punches of 1.5 cm^2, stored at -18^{o}C, were extracted in 20 mL of ultrapure water upon sonication (ultrasonic sonicator Elmasonic S80) for 30 min. Subsequently, the extracts were placed in a syringe pump which was operated at a flow rate of 15 mL hr^{-1}. Upon atomization, the generated water droplets passed through a silica gel dryer and the produced aerosol was then analyzed by a HR-ToF-AMS (Aerodyne Inc.). The AMS measurements lasted for 30 min, in order to collect 10 AMS scans (each scan required 3 min for completion). Prior to sample analysis and in-between samples, blanks of ultrapure water were analyzed for 30 min. The blank spectra were used for correction of the ambient sample spectra. In total, 48 filter samples were analyzed and the corresponding OA spectra were analyzed using positive matrix factorization (PMF) to derive the relative contributions of the various factors. The absolute concentrations of each factor were estimated by multiplying the factor contributions from the off-line AMS analysis with the absolute OA concentrations measured by the other techniques.

The SoFi (Source Finder) version 8.5 was used for the PMF analysis. Details of the procedure followed can be found in Vassilakopoulou et al. (2022). In brief, F_{peak} values ranging from -1 to 1, with a 0.1 step were tested. The optimum F_{peak} was selected in accordance with the physical meaning of the factors, the resulting spectral profiles, and their correlation with other measurements. Two, three and four factor solutions were examined for the source apportionment analysis. The two-factor solution indicated an oxygenated (OOA) and a primary organic aerosol (HOA) factor with the OOA contributing 65% of the OA. In the four-factor solution, two factors represented OOA spectra, while one represented a primary source. The fourth factor was not identifiable, as its spectrum did not resemble any reference factors (all examined reference factors had a high theta angle (>60o) with the fourth factor). Thus, the four-factor solution was rejected. Finally, the three-factor solution was the optimum choice, as it reproduced significantly better the variation of the OA spectra during the study compared to the two-factor solution.

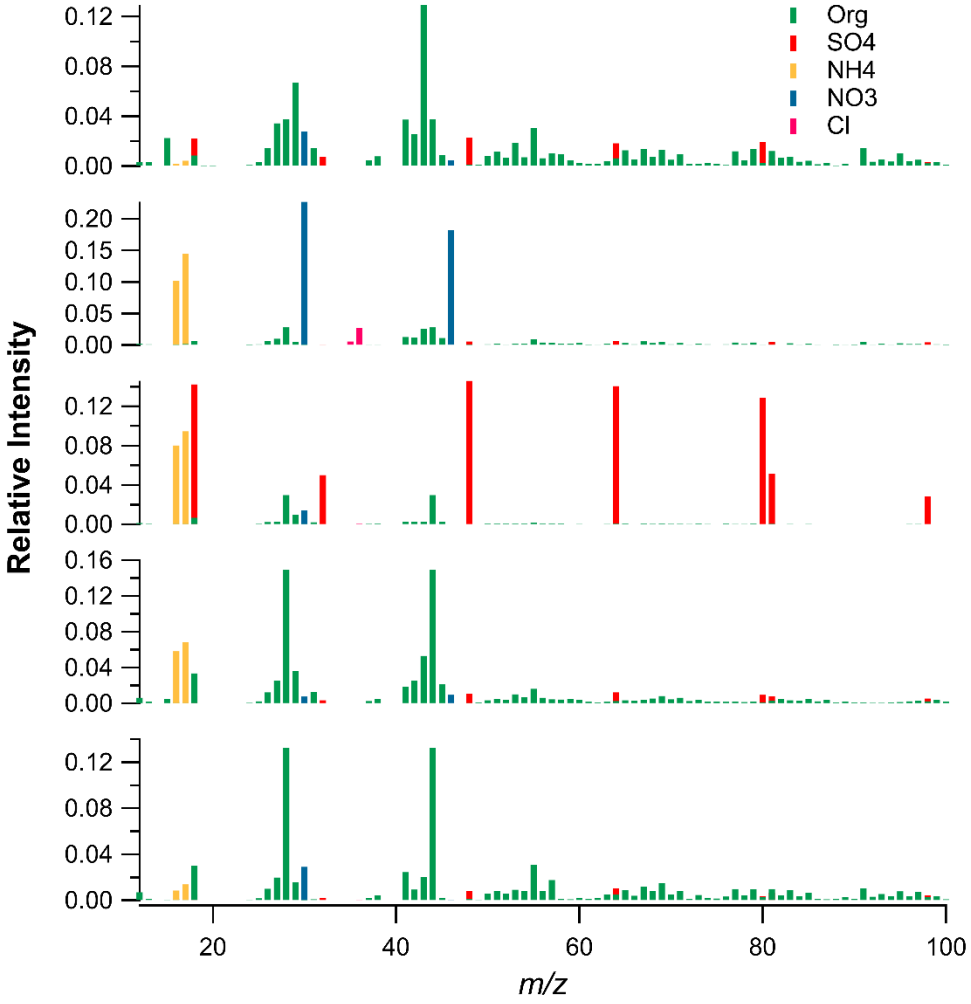

Figure S4. Mass spectra of the five PM1 factors.

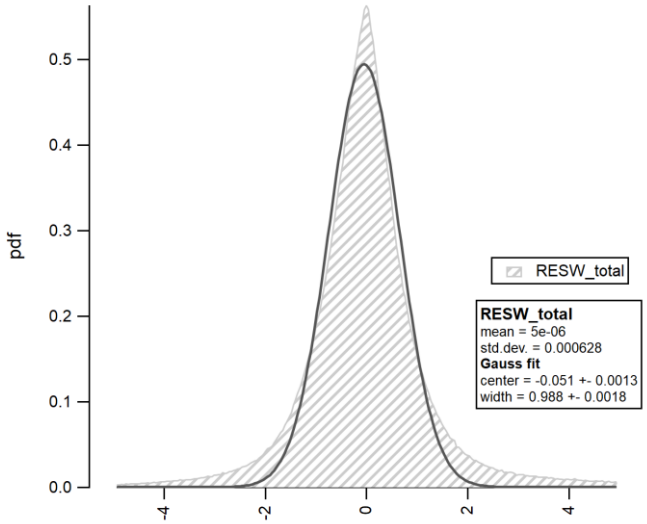

Figure S5. PDF of scaled residuals for the combined PMF solution

100

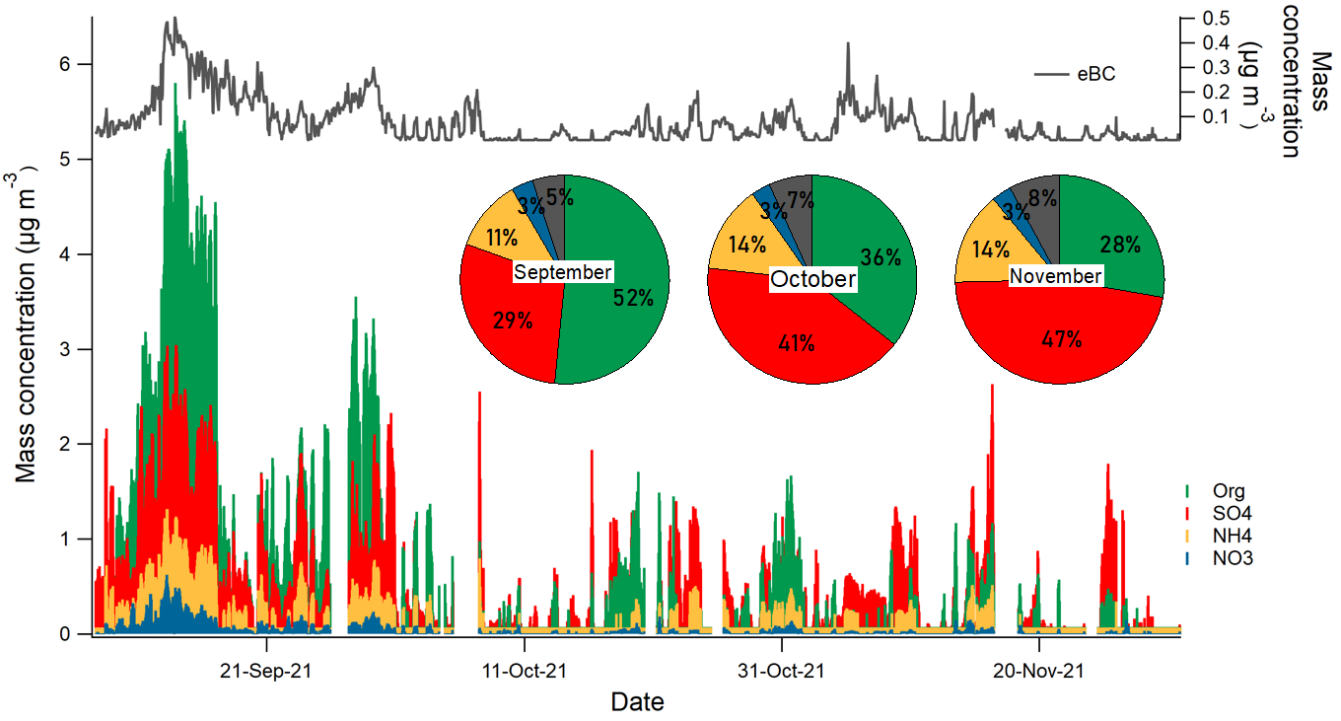

105 **Figure S6. Time series of non-refractory species as measured by the ToF-ACSM (organics: green, sulphate: red, ammonium: yellow and nitrate: blue) and *eBC* (grey) for the campaign period and pie charts indicating the mass fraction and mass concentration of each PM_1 component for each month: September, October and November.**

110

115

120

Table S1. Average mean concentration of ACSM species and eBC during the campaign and monthly.

μg m^{-3} / %	*Org*	*SO_4*	*NH_4*	*NO_3*	*eBC*	*Total PM_1*
September	1.86 / 52	1.04 / 29	0.39 / 11	0.12 / 3	0.17 / 5	3.6
October	0.31 / 36	0.35 / 41	0.12 / 14	0.03 / 3	0.04 / 7	0.8
November	0.19 / 28	0.32 / 47	0.10 / 14	0.02 / 3	0.05 / 8	0.7
Campaign average	0.68 / 44	0.53 / 35	0.19 / 12	0.05 / 3	0.08 / 5	1.6

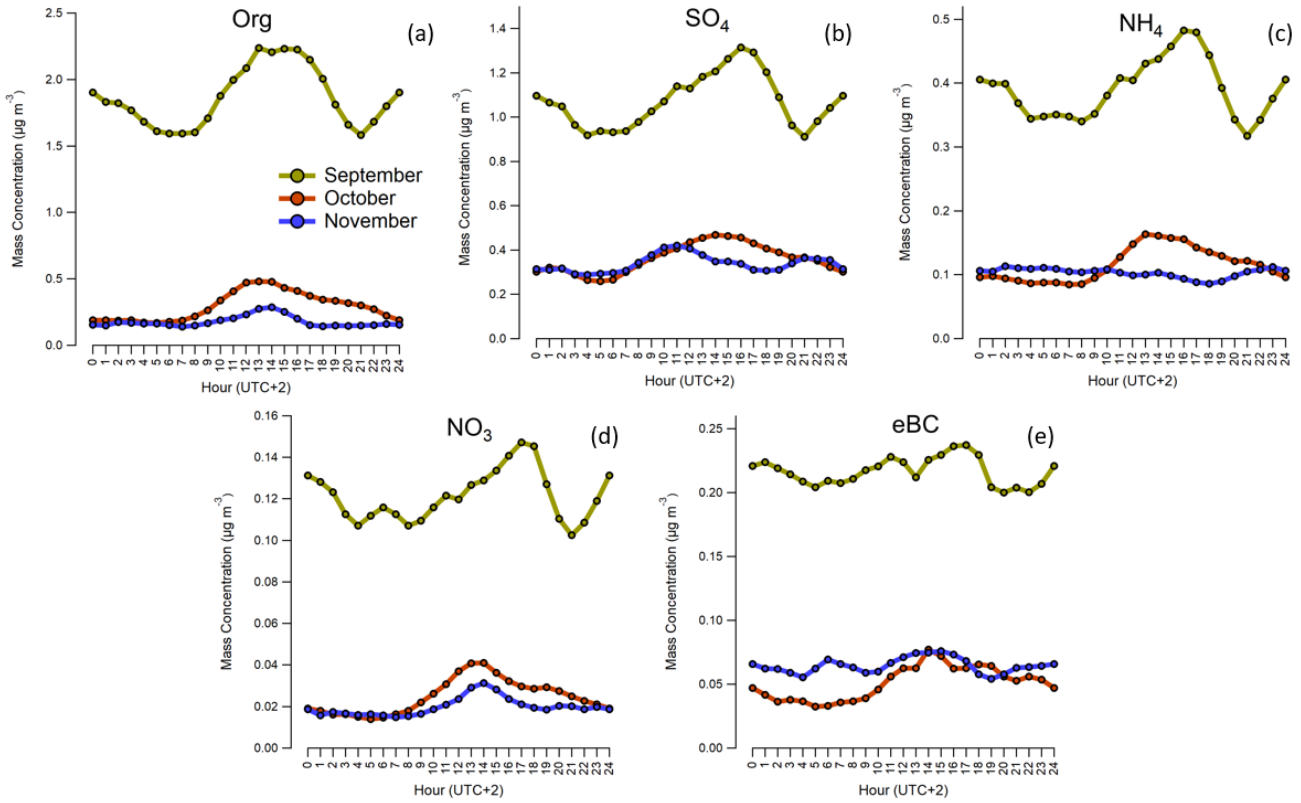

Figure S7. Diurnal profiles of the five species: organics (a), sulphate (b), nitrate (c), ammonium (d) and *eBC* (e) for each month of the campaign in UTC+2.

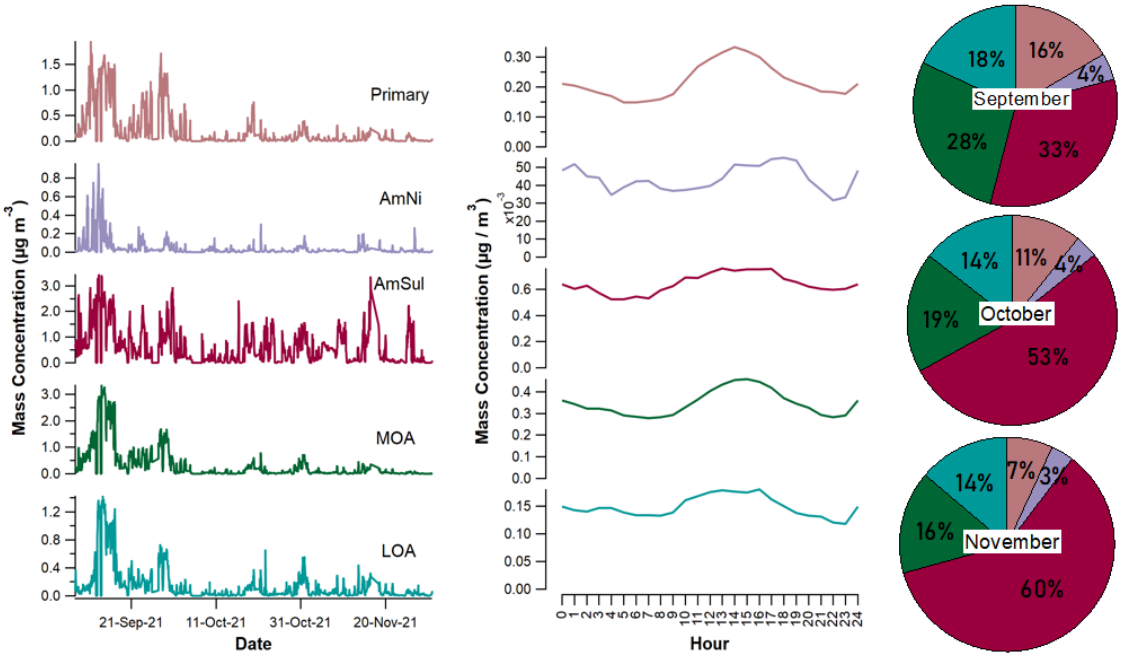

Figure S8. Time series, diurnal profiles (in UTC+2) and relative contribution of each PMF factor.

Table S2. R-Pearson correlation of POA with external tracers

R-Pearson	*POA*
eBC	0.74
Total number concentration	0.66
Aitken mode volume	0.65
Accumulation mode volume	0.72
CO	0.55
NH_4	0.85
SO_4	0.77
NO_3	0.84

Table S3. Monthly averaged mass concentration and composition of the factors resolved

% / µg m^{-3}	*POA*	*AmNi*	*AmSul*	*MOA*	*LOA*	*Sum*
September	0.54 / 16	0.14 / 4	1.09 / 33	0.92 / 28	0.59 / 18	3.2
October	0.08 / 11	0.03 / 4	0.38 / 53	0.13 / 19	0.1 / 14	0.7
November	0.04 / 7	0.02 / 3	0.35 / 60	0.09 / 16	0.08 / 14	0.6
Campaign average	0.19 / 14	0.06 / 4	0.57 / 41	0.33 / 24	0.23 / 17	1.4

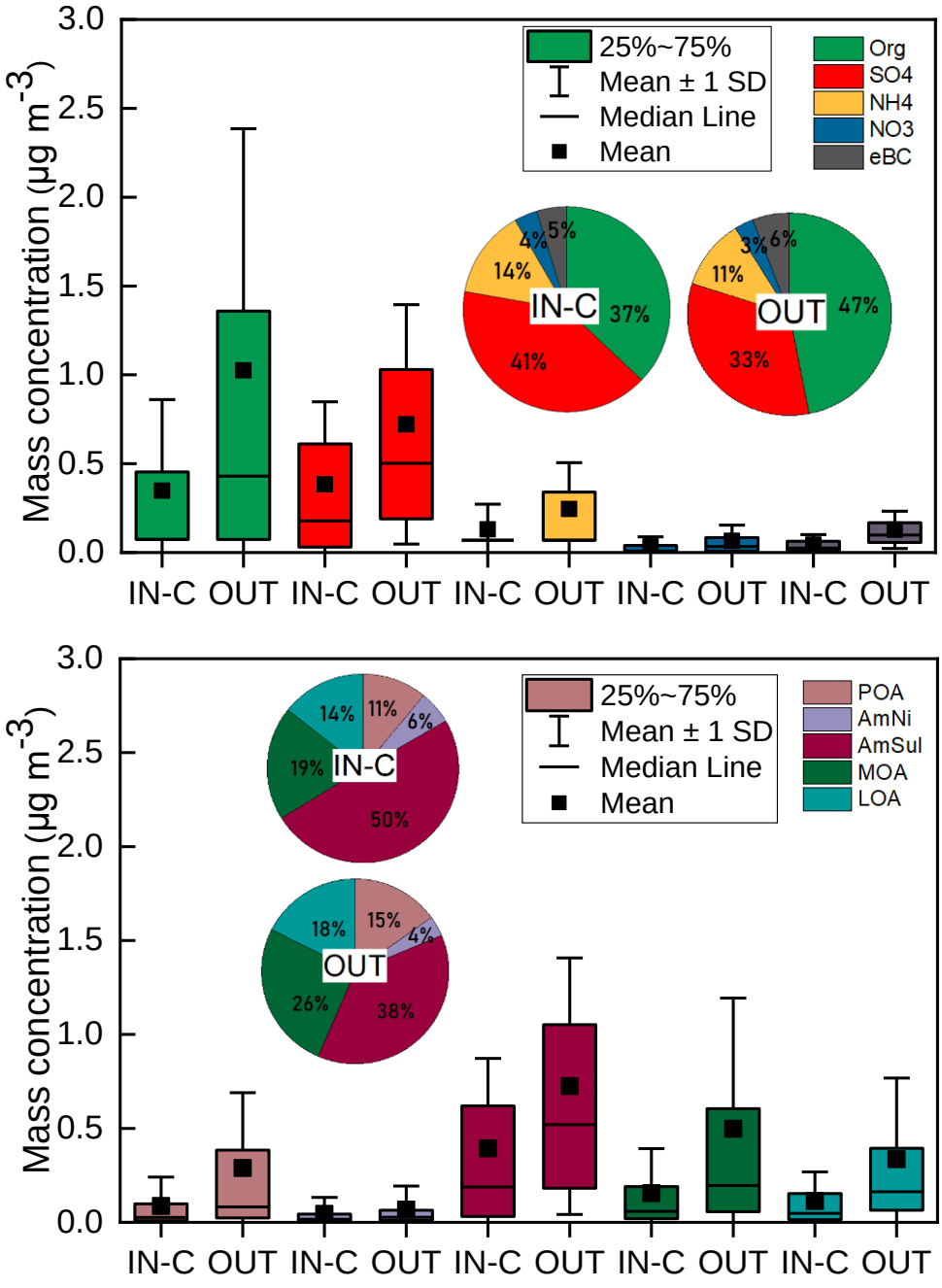

205 **Figure S9. Box plots and relative contribution of each NRS and *eBC* (a) and each PMF factor (b) in cloud periods (IN-C) and under non-cloud (OUT) conditions. The boxes range are the 25th and 75th percentiles, while the whiskers ranges are the ±Standard Deviation. The median is described as a horizontal line, while the rectangular represents the average value.**

Table S4. Average values of PM_1 species and PMF factors in cloud periods (IN-C) and under non-cloud (OUT) conditions

Average Concentration ($\mu g\ m^{-3}$)	*IN-C*	*OUT*	*Average Concentration ($\mu g\ m^{-3}$)*	*IN-C*	*OUT*
Organics	0.35	1.03	***POA***	0.09	0.29
SO_4^{2-}	0.38	0.72	***AmNi***	0.04	0.07
NH_4^+	0.13	0.25	***AmSul***	0.39	0.72
$NO3^-$	0.03	0.07	***MOA***	0.15	0.5
eBC	0.04	0.13	***LOA***	0.11	0.34
Total PM_1	0.95	2.19	***Total PMF***	0.79	1.91

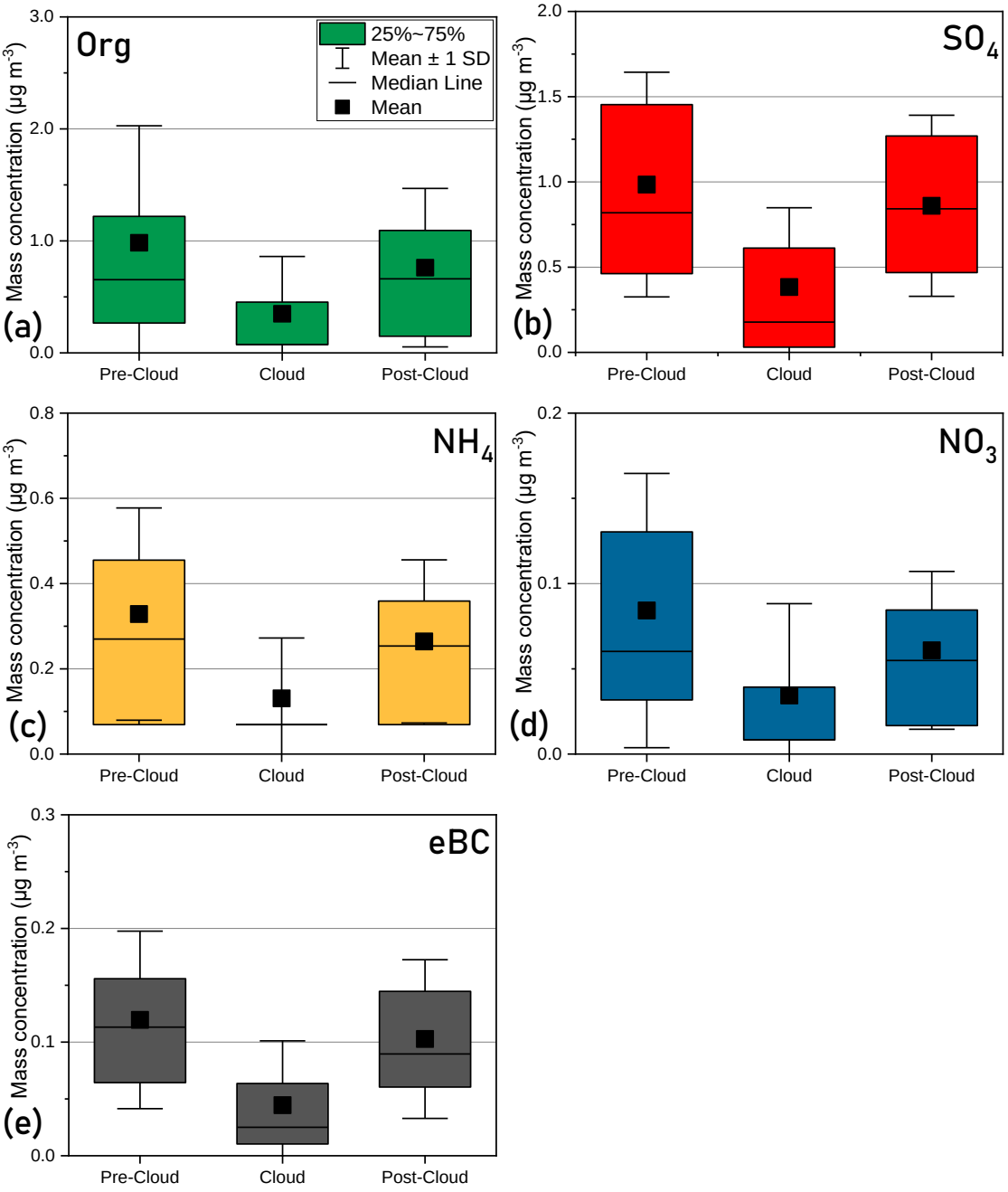

Figure S10. Organics (a), SO_4 (b), NH_4 (c), NO_3 (d) and *eBC* (e) box plots for pre-cloud, cloud and post-cloud conditions. The boxes range are the 25th and 75th percentiles, while the whiskers ranges are the ±Standard Deviation. The median is described as a horizontal line, while the rectangular represents the average value.

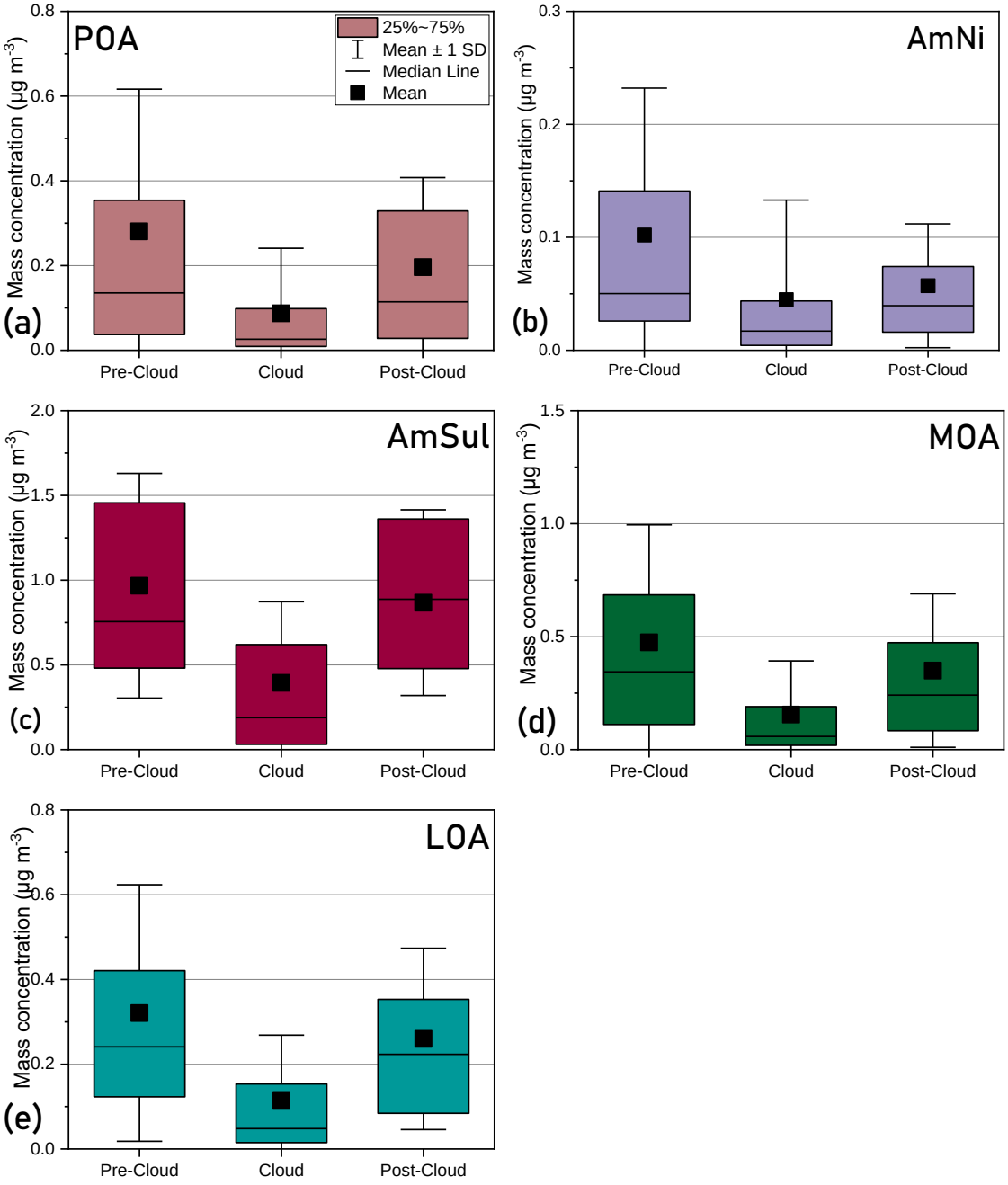

Figure S11. POA (a), AmNi (b), AmSul (c), MOA (d) and LOA (e) box plots for pre-cloud, cloud and post-cloud conditions. The boxes range are the 25th and 75th percentiles, while the whiskers ranges are the ±Standard Deviation. The median is described as a horizontal line, while the rectangular represents the average value.

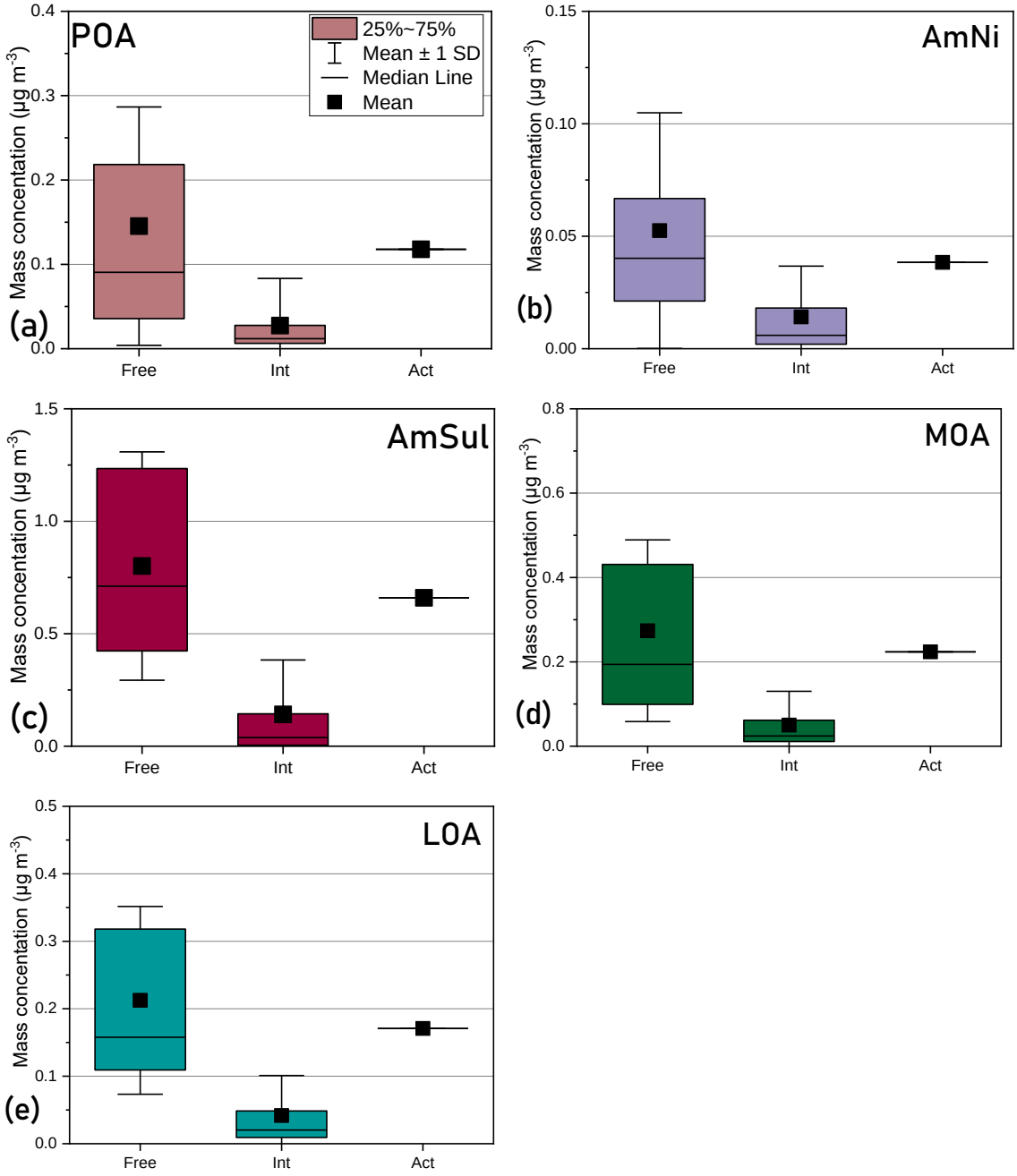

Figure S12. POA (a), AmNi (b), AmSul (c), MOA (d) and LOA (e) box plots for cloud-free (1 hour before cloud formation) (Free), interstitial (Int) and activated aerosol (only the average value as the difference between the mass concentration before cloud formation minus the mass concentration of the interstitial part of the aerosol) (Act). The boxes range are the 25th and 75th percentiles, while the whiskers ranges are the ±Standard Deviation. The median is described as a horizontal line, while the rectangular represents the average value.

Table S6. Average values of PM_1 species and PMF factors for PBL and FT conditions

Average Concentration ($\mu g\ m^{-3}$)	*PBL*	*FT*	*Average Concentration ($\mu g\ m^{-3}$)*	*PBL*	*FT*
Organics	1.3	0.22	***POA***	0.37	0.06
SO_4^{2-}	0.91	0.16	***AmNi***	0.09	0.01
NH_4^+	0.3	0.08	***AmSul***	0.92	0.15
$NO3^-$	0.08	0.01	***MOA***	0.63	0.10
eBC	0.15	0.05	***LOA***	0.42	0.07
Total PM_1	2.75	0.52	***Total PMF***	2.43	0.41

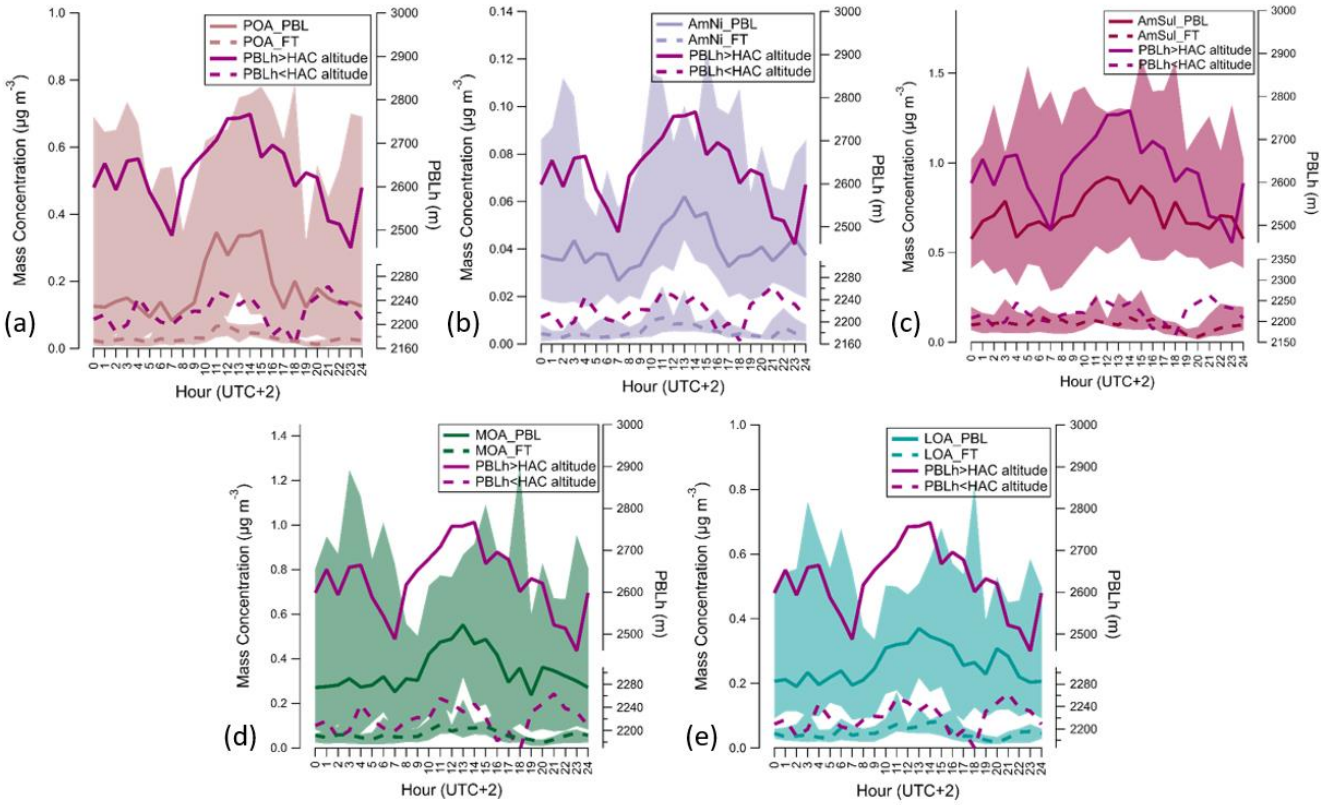

Figure S13. Median and interquartile (10th and 90th) diurnal trends for each PMF factor (a: POA, b: AmNi, c: AmSul, d: MOA and e: LOA) for the whole campaign segregated between PBL-influenced days and days in the FT based on the criterion of at least 2 methods.

265

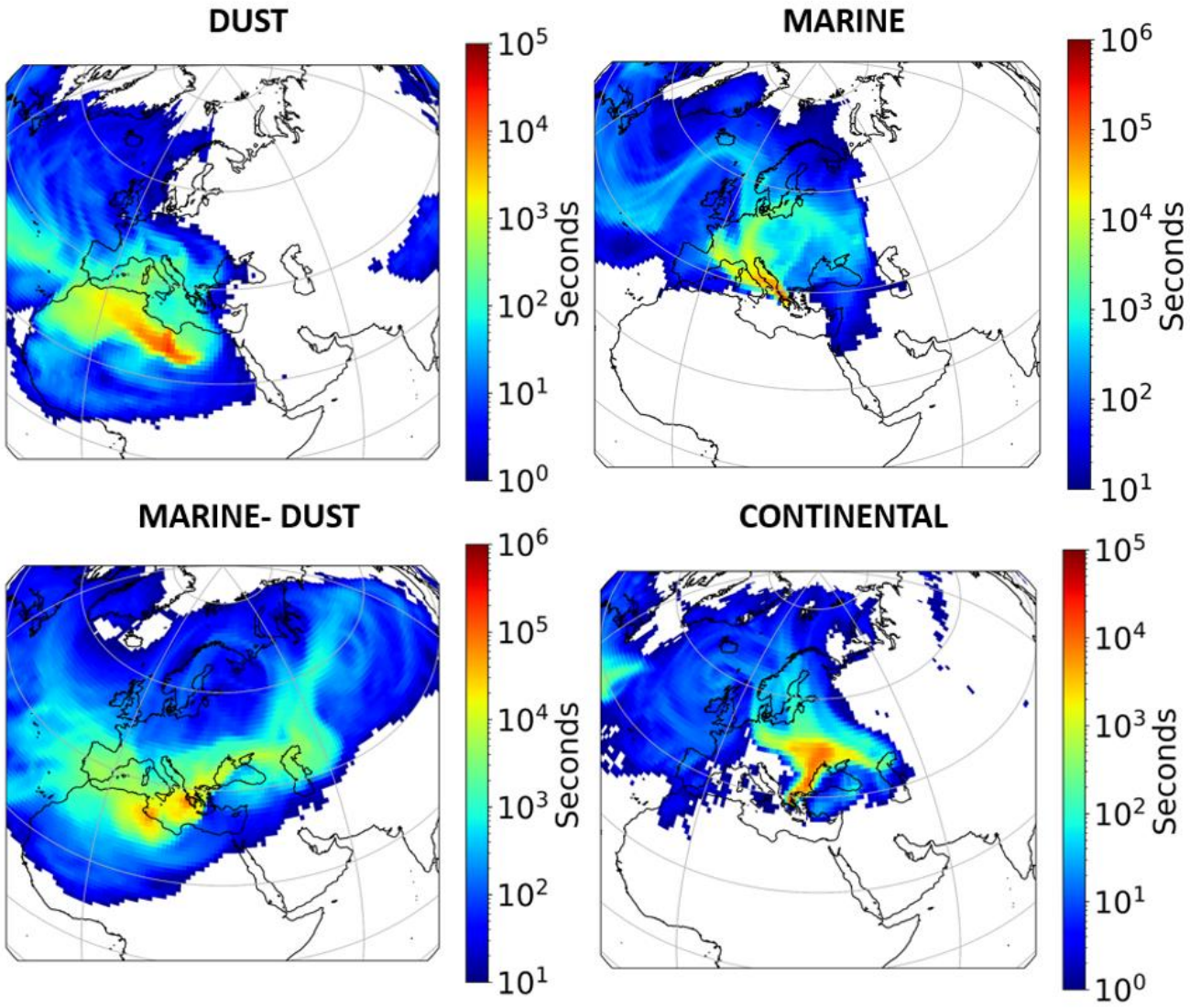

Figure S14. Prevailing air mass origins during CALISHTO as obtained from FLEXPART divided in Dust when incoming from the North of Africa (D), Marine-Dust when originating from the North Africa trespassing through the Adriatic or the Mediterranean Sea (M-D), Marine from the Adriatic or the Mediterranean Sea (M) and Continental from the continental Europe (C).

270